Chapter 2
Nanomechanical Cantilever-Based Manipulation for Sensing and Imaging

Nader Jalili

Abstract This brief chapter provides an overview of nanomechanical cantilever (NMC) systems with their applications in cantilever-based imaging and manipulation platforms such as atomic force microscopy (AFM) and its varieties. Some new concepts in modeling these systems are also introduced along with practical applications in laser-free imaging and nanoscale manipulation and positioning. In an effort to keep this chapter focused, only a brief overview of these topics is presented in this chapter. Finally, the outlook in NMC-based imaging and manipulation is given.

2.1 Classification of Control and Manipulation at the Nanoscale

Advancement of emerging nanotechnological applications such as nanoelectromechanical systems (NEMS) require precise modeling, control and manipulation of objects, components and subsystems ranging in sizes from few nanometers to micrometers. The added complexity of uncertainties and nonlinearities at nanoscale combined with the sub-nanometer precision requirement calls for the development of fundamentally new techniques and controllers for these applications. This area of research has recently received widespread attention in different technologies such as fabricating electronic chipsets, testing and assembly of MEMS and NEMS, micro-injection and manipulation of chromosomes and genes [1]. For example, in nanofiber manipulation, the ultimate goal is to grasp, manipulate and place nanofibers in certain predefined arrangement (see Fig. 2.1). Other applications could include defining materials properties, fabricating electronic chipsets, testing

N. Jalili (✉)
Department of Mechanical and Industrial Engineering, 334 Snell Engineering Center, Northeastern University, 360 Huntington Avenue, Boston, MA 02115, USA
e-mail: n.jalili@neu.edu

C. Mavroidis and A. Ferreira (eds.), *Nanorobotics*, DOI 10.1007/978-1-4614-2119-1_2,

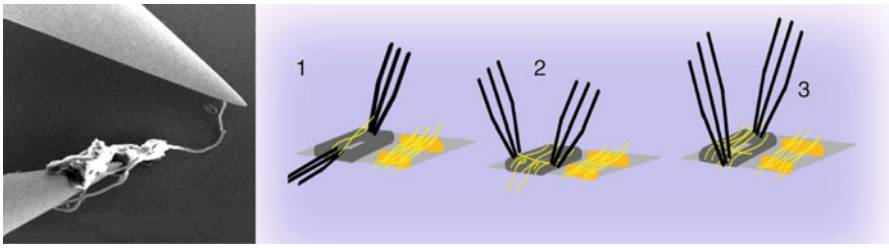

Fig. 2.1 (*Left*) Manipulation of nanofiber using MM3A® Nanorobot from Kleindiek®, (*right*) schematic representation of automated weaving process; (1) placement of the fibers and folding in the warp direction, (2) fiber placement in the weft, and (3) unfolding of the warp. Reprinted with permission

microelectronics circuits, assembly of MEMS and NEMS, teleoperated surgeries, microinjection, as well as manipulation of chromosomes and genes.

In general, nanoobject manipulation is defined as grasping, manipulating and placing nanoobjects in certain predefined arrangement. The strategies for control and manipulation at the nanoscale can be divided into the following two general categories:

1. Scanning probe microscopy (SPM)-based techniques
2. Nanorobotic manipulation (NRM)-based techniques

Under the first category, the following platforms can be utilized: scanning tunneling microscope (STM) and nanomechanical cantilever (NMC)-based systems (e.g., atomic force microscopy, AFM). On the other hand, NRM-based systems are more flexible and versatile in nanoscale manipulations. However, due to complexity and difficulty in sensing requirements (e.g., low-speed imaging acquisition and capturing in scanning electron microscopy (SEM) systems), control and manipulation using these systems might be limited, and hence, not discussed here.

2.1.1 Scanning Probe Microscopy-Based Control and Manipulation

In SPM systems, a probe is scanned over the surface at a small distance, where an "*interaction*" between the probe and the surface is present. This interaction can be of various nature (e.g., electrical, magnetically, mechanical) and provides the measured signal (tunnel current, force, etc.), see Fig. 2.2. SPM systems have numerous applications in a variety of disciplines and fields such as materials science, biology, chemistry, and many more areas.

As mentioned earlier and depicted in Fig. 2.2, under SPM-based control and manipulation techniques, STM and AFM platforms are referred to as the two most widely accepted techniques. As a matter of fact, early efforts on nanomanipulation

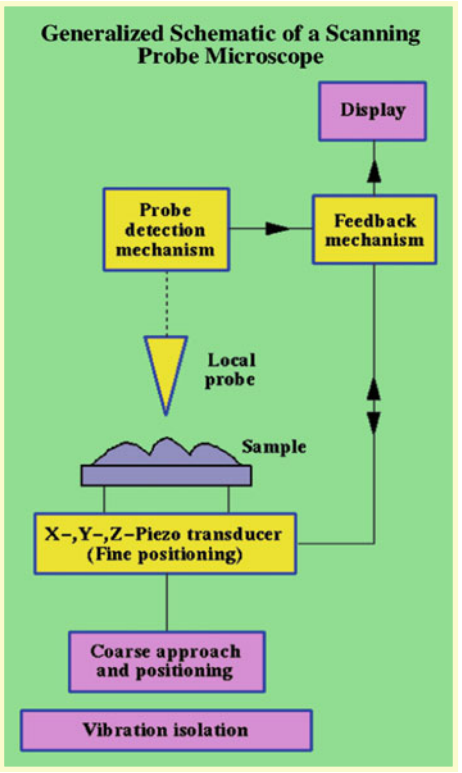

Fig. 2.2 Generalized schematic of scanning probe microscopy (SPM) system. Reprinted with permission

were initiated by both STM [2] and AFM [3]. Other techniques such as optical tweezers [4] and magnetic tweezers [5] have been also used for this purpose. Although this chapter focuses on NMC-based imaging/manipulation platform, other techniques are briefly reviewed to provide a comparative basis.

2.1.1.1 Scanning Tunneling Microscope, an Electrical SPM-Based Control and Manipulation

The STM, invented in 1982 by Binnig and Rohrer [2], was originally designed to perform real space atomic resolution imaging of a material's surface. The ability to obtain atomic resolution images with the STM arises from its unique operating principles. The microscope uses a sharp, metallic tip that is placed only a few Angstroms (10^{-10} m) from a conducting surface. At this distance, the tip conducts tunneling electrons or "tunnel current" from the surface and probes the surface electron density at that point. The electron density is exponentially dependent on the tip-surface separation, which makes the tunnel current a highly sensitive measure of this relative distance.

The strong interactions that can exist between a scanning tip and atoms/molecules at the surface can lead to alterations in surface chemical structure and, if controlled properly, can be used to move atoms or molecules and build nanoscale structures. It is this feature of the STM that forms the basic concept in nanomanipulation, i.e., due to its ultrahigh imaging resolution, nanoparticles as small as atoms can be manipulated.

2.1.1.2 Atomic Force Microscope, an Electromechanical SPM-Based Control and Manipulation

As mentioned earlier, AFM systems belong to the category of NMC-based systems, a subcategory of SPM systems. A typical AFM system consists of a micromachined cantilever probe with a sharp tip that is mounted to a piezoelectric actuator with a position-sensitive photo detector that receives a laser beam reflected off the back of the AFM tip. Roughly speaking, AFM is operated by moving the sample under the AFM tip and then recording the vertical displacement of the tip as the samples moves. As the AFM tip hovers across the surface of the sample, the tip moves up and down with the contour of the surface. A laser beam, deflected off the back of the AFM tip, is captured by a detector. This laser/detector configuration could provide displacement measurements that are utilized to generate topographical images and to control the piezoelectric actuators.

The AFM system has evolved into a useful tool for direct measurements of microstructural parameters and the intermolecular forces at the nanoscale level. Similar to STM, AFM system can also be used for manipulation at the nanoscale. In manipulation via AFM in non-contact mode, the image of nanoparticle is taken, the tip oscillation is removed and the tip is approached to particle while maintaining contact with the surface. In manipulation via AFM, larger forces can be applied to the nanoparticle and any object with arbitrary shape can be manipulated in 2D space. However, the manipulation of individual atoms or nanofibers with an AFM is still a major challenge and practically difficult task [6].

2.1.2 Nanorobotic Manipulation-Based Control and Manipulation

In manipulation via NRMs, much more degrees of freedom (DOFs) including rotation for orientation control of nanoparticle are feasible. For this reason, NRMs can be used for manipulations in 3D space. However, the relatively low resolution of electron microscope in manipulation with NRMs is a limiting factor in this nanomanipulation. A NRM system generally utilizes nanorobot as the manipulation device, microscopes or CCD camera as visual feedback, end-effectors including cantilevers and tweezers or other type of SPM and some sensors (e.g., force, displacement, tactile and strain) to manipulate nanoparticles [6].

Fig. 2.3 MM3A nanomanipulator [7], reprinted with permission

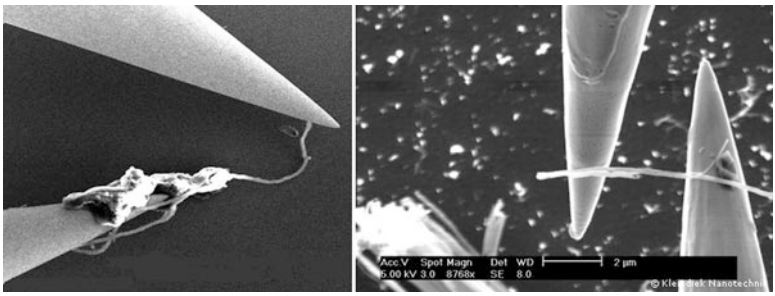

Fig. 2.4 MM3A manipulating nanofibers under scanning electron microscope (SEM). *Source*: [7], reprinted with permission

Among the variety of available NRM-based configurations, an attractive platform is a 3DOF nanomanipulator. This nanomanipulator, named as MM3A® and depicted in Fig. 2.3, consists of two rotational motors and one linear Nanomotor® [7]. The MM3A travels a distance of 1 cm within a second, with up to 1nm step precision. Using a single drive system, it integrates both coarse and fine manipulations [5]. It also offers a high degree of flexibility, that is, the nanomanipulator is capable of approaching a sample at any angle along the *X*, *Y* and *Z*-axes [7, 8].

As mentioned earlier, one attractive application of NRMs is to manipulate nanofibers, weave and utilize them in a variety of textile-related applications (see Fig. 2.4). The MM3A nanomanipulator combined with a novel fused vision force feedback controller can be utilized to address such a critical need in nano-fabric production automation [8–11].

2.2 Nanomechanical Cantilever-Based Imaging

As mentioned in the preceding subsection, AFM serves as one of the most effective tools in imaging at the nanoscale. In an effort to reduce the cost and improve the speed of AFM in molecular scale imaging of materials, a laser-free AFM proposition augmented with an accurate control strategy for its scanning axes is presented here. To replace the bulky and expensive laser interferometer, a piezoresistive sensing device with an acceptable level of accuracy is employed. Change in the resistance of piezoelectric layer due to the deflection of microcantilever, caused by the variation

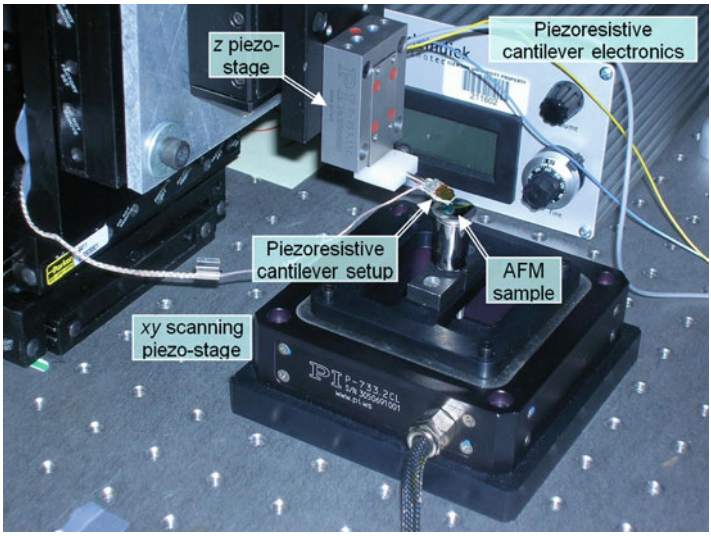

Fig. 2.5 Piezoresistive cantilever-based laser-free AFM setup. *Source*: [13], reprinted with permission

of surface topography, is monitored through a Wheatstone bridge. Hence, the surface topography is captured without the use of laser and with nanometer scale accuracy.

2.2.1 A NMC-Based Laser-Free AFM System for Fast Imaging

Figure 2.5 depicts the proposed laser-free AFM setup. The sample to be imaged is mounted on the double-axes parallel piezo-flexural stage, while a piezoresistive microcantilever is mounted on another piezoelectric z-stage for acquiring sample topography. The z-stage is used only for the initial adjustment and to bring the cantilever into a desired contact with the sample. During scanning, z-stage does not move; hence, the cantilever deflection corresponds to the surface topography (see Fig. 2.6 for the schematic view of laser-free AFM setup).

A self-sensing microcantilever, PRC-400, is utilized here for imaging purpose. Figure 2.7 depicts the piezoresistive cantilever image under a 100× magnification light microscopy consisting of a silicon microcantilever with a piezoresistive layer on its base, a sharpened tip, and a piezoresistive reference lever. The piezoresistive layers on cantilever and reference lever are utilized as resistances in a Wheatstone bridge. Due to the external force on the piezoresistive cantilever's tip, it bends and results in a change of resistance in the piezoresistive layer. This change of resistance can be monitored utilizing the output voltage of the Wheatstone bridge. Figure 2.7 depicts a schematic of the PRC-400 self-sensing cantilever, with external

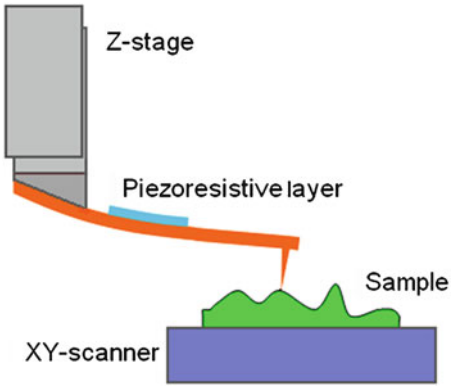

Fig. 2.6 Schematic representation of laser-free AFM setup. *Source*: [13], reprinted with permission

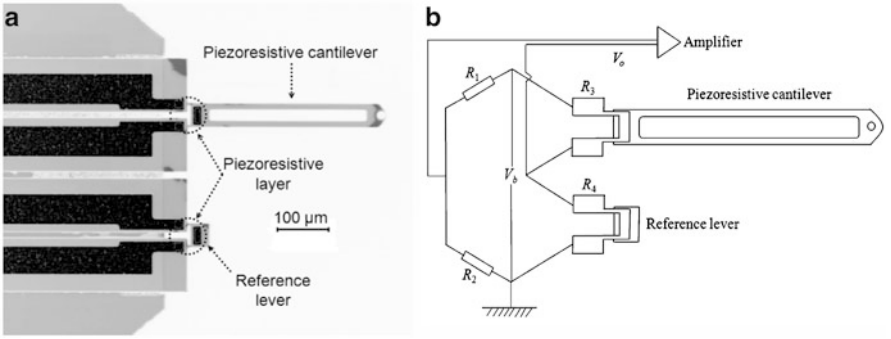

Fig. 2.7 Piezoresistive microcantilever with Weston bridge circuit. *Source*: [12], reprinted with permission

Wheatstone bridge and amplifier. The relation between the cantilever deflection and output voltage of the Wheatstone bridge is typically linear [12]. Thus, the cantilever deflection can be estimated through the deflection-to-voltage gain of the piezoresistive cantilever.

At the tip/sample contact point, the magnitude of the force applied to the cantilever tip is equally the same as the magnitude of the force applied to the sample surface. Cantilever's dimensions are, however, extremely small, and it only undergoes bending. Hence, the high flexibility of the cantilever is realized compared to the sample that distributes the force around the contact point and resists against it. As a result, the vertical deformation of sample at the contact point becomes negligible compared to that of the cantilever. This assumption is valid unless ultrasoft samples (e.g., liquids, soft biological species or ultrathin polymeric layers) are under study. Within the scope of this chapter, only stiff enough samples are addressed. Imaging ultrasoft samples requires further experiments to identify the local stiffness of the material, and is better done using non-contact or tapping AFM modes. On the other hand, the variation of surface topography in contact mode AFM

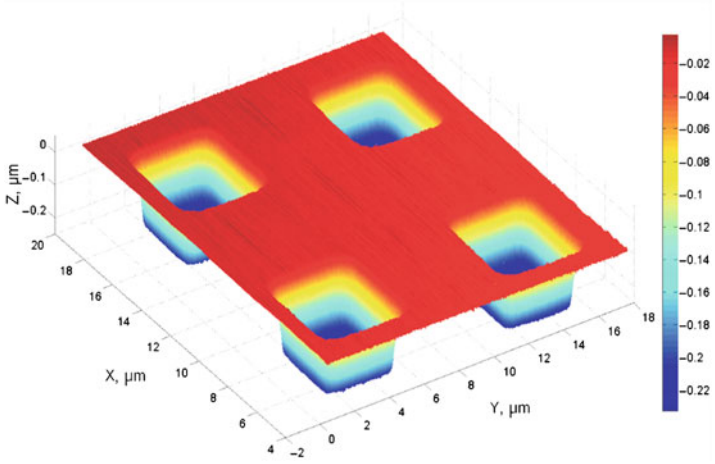

Fig. 2.8 3D image of an AFM calibration sample with 200nm steps captured by the developed laser-free AFM setup at 10 Hz raster scanning. *Source*: [13], reprinted with permission

should not exceed a certain value beyond which the cantilever would experience plastic deformation or yield. Since the length of a typical AFM cantilever is in the order of several hundred micrometers, it can safely bend for few tens of microns. This flexibility is sufficient for most of the current AFM applications with micro- and nano-scale topographical variations.

2.2.2 *Development of a Robust Adaptive Controller for Laser-Free Imaging*

Utilizing a robust adaptive controller for *x*–*y* nano-positioner, an AFM calibration sample with 5×5 μm^2 cubic pools with 200nm depth, uniformly distributed on its surface, is considered for the experimental implementation of the proposed laser-free AFM setup. Figure 2.8 demonstrates the 3D image of the sample within a 16×16 μm^2 scanning area at 10 Hz scanning frequency. It is particularly desired to observe the quality of images acquired in different scanning speeds (or in the other words, scanning frequencies). Figure 2.9 demonstrates the top view of images at frequencies varying from 10 to 60 Hz with 10 Hz increments. It is seen that as the frequency increases, the quality drops and images become more blurry. This effect could have been originated from the increased transversal vibrations of microcantilever due to facing with the steeper steps in the surface at higher speeds, and/or the sensitivity reduction of piezoresistive layer due to the frequency increase. Further information such as cross-sectional view (line scan) of the surface could yield better judgment in this regard.

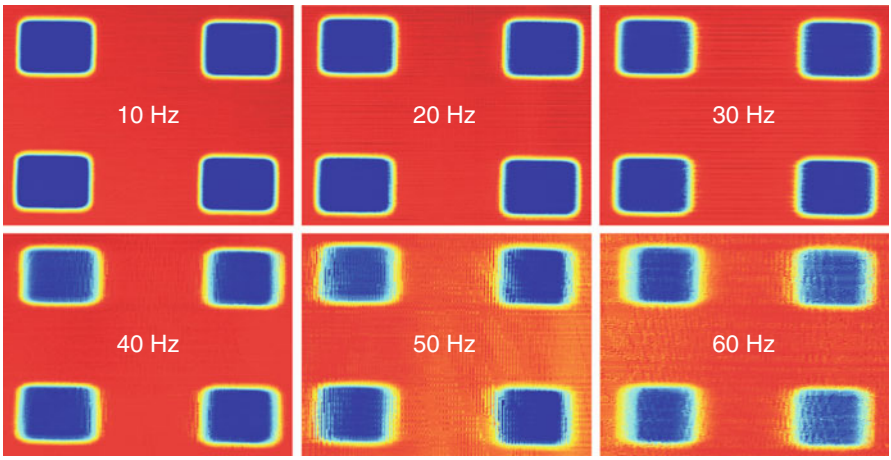

Fig. 2.9 Effects of raster scanning frequency on the image quality of laser-free AFM. *Source*: [13], reprinted with permission

As seen from Fig. 2.9, it reveals that at frequency of 30 Hz or less, the steep topographical steps are captured clearly by the cantilever and its piezoresistive sensor. However, when the frequency increases to 40 Hz and more, the stepped edges seem smoother and the image loses accuracy around the step areas. Moreover, at high frequencies, particularly at 60 Hz, the measured topography finds a negative slope which leads to further accuracy loss. Both of these effects cannot originate from the cantilever's vibrations, neither can they come from cantilever's irresponsiveness. This is due to the ultrahigh natural frequency of microcantilevers (in the order of several kHz) which significantly reduces their rise time and makes them extremely responsive. Hence, we may conclude that the degradation of image at high frequencies is due to the deficiency of the piezoresistive measurement at high frequencies which sets the limit to the proposed laser-free AFM device. Hence, one of the important future directions of piezoresistive-based AFMs would be improving the accuracy of piezoresistive sensors through their manufacturing process and electronics integration.

Nevertheless, acquiring high-quality images at frequencies up to 30 Hz could imply the effectiveness of the proposed control framework in increasing the speeds of current AFMs which typically suffer from the low speed of commonly used PID controllers.

2.3 Nanomechanical Cantilever-Based Manipulation

A relatively common manipulation configuration using AFM is to maintain a desired force, mostly constant, at the cantilever tip. Hence, the control objective is to move the cantilever base in order to acquire this desired force at the tip. This

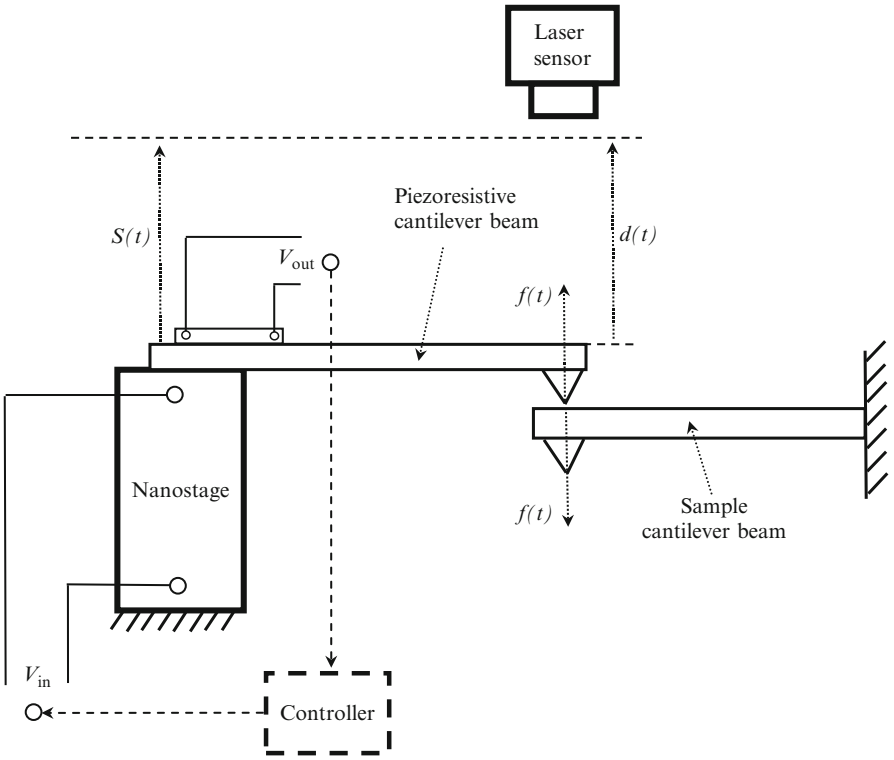

Fig. 2.10 Schematic of the NMC-based force sensing experimental setup. *Source*: [12], reprinted with permission

is a highly demanding mission in nanomanipulation and imaging; for instance, in contact imaging in AFM, there is a need to keep the force at the cantilever's tip in a constant value [12, 14]. Moreover, in almost all of the non-destructive materials characterization and nanomanipulation tasks, there is a need to control the interaction force between the cantilever's tip and the surface or nanoparticle.

2.3.1 *Nanoscale Force Tracking Using NMC-Based Manipulation*

Figure 2.10 depicts the schematic of such nanoscale force tracking using a piezoresistive cantilever with a PZT-actuated base. The objective here is to sense the force acting on the piezoresistive cantilever's tip utilizing the output voltage of the piezoresistive beam and smoothly move its base to acquire the desired force on the piezoresistive cantilever's tip. The control objective is to obtain the desired force at the cantilever's tip, which is measured utilizing the output voltage of the

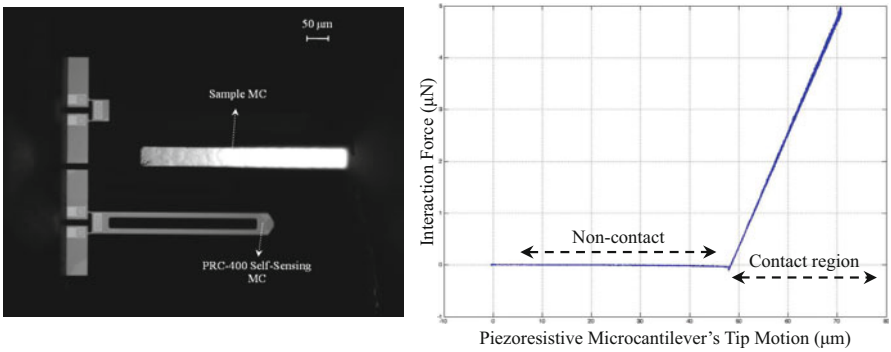

Fig. 2.11 (*Left*) Experimental setup of pushing sample NMC with piezoresistive NMC, and (*right*) the interaction force between sample and piezoresistive NMCs. *Source* (for the left figure only): [12], reprinted with permission

piezoresistive layer, V_{out}. Acquiring the force acting on the tip, this force and the desired value for the force are fed back to the controller that generates the suitable control command and sends it to the nanostage as the input voltage V_{in}.

2.3.2 Controlled Tip Force-Based Manipulation

A set of experimental results are presented for tracking a desired nanoscale force at the tip of NMC. For this, the piezoresistive NMC is brought close to a sample NMC (see Fig. 2.11, left) and the output voltage from piezoresistive layer is utilized to predict the force acting on the NMC's tip. By comparing the predicted force with the desired trajectory, the error which should be regulated can be easily determined. However, in order to identify the actual force acting on the NMC and compare it with the estimated force through the modeling, another measurement mechanism is employed using a laser-based measurement technique, for instance. Figure 2.11, right depicts the experimental results to identify the sample NMC's stiffness. The slope of the line depicted in Fig. 2.11, right in the contact region represents the force acting on the sample NMC's tip over the sample NMC's deflection which is also the sample NMC's stiffness. Utilizing the sample NMC's stiffness and its deflection, the actual force acting on the NMC's tip can be determined.

2.4 Summary

This chapter briefly provided a relatively general overview of NMC-based imaging and manipulation systems with their applications in many cantilever-based systems such as AFM and its varieties. It specifically presented some new concepts in

imaging at the nanoscale using laser-free setup and highlighted the issues related to nonlinear effects at such small scale, piezoelectric materials nonlinearity and remedies for control at these scales. The concepts of NMC-based manipulation and tip force-based control were presented with their applications in numerous biological species manipulation, cell mechanics and ultrasmall mass sensing and detection.

References

1. Kallio P, Koivo HN (1995) Microtelemanipulation: a survey of the application areas. In: Proceedings of the international conference on recent advances in mechatronics. ICRAM'95, Istanbul, August 1995, pp 365–372
2. Binnig G, Rohrer H, Gerber C, Weibel E (1982) Surface studies by scanning tunneling microscopy. Phys Rev Lett 49:57–61
3. Binnig G, Quate CF, Gerber C (1986) Atomic force microscope. Phys Rev Lett 56:93–96
4. Ashkin A, Dziedzic JM, Bjorkholm JE, Chu S (1986) Observation of a single-beam gradient force optical trap for dielectric particles. Opt Lett 11:288–290
5. Crick FHC, Hughes AFW (1950) The physical properties of cytoplasm: a study by means of the magnetic particle method. Exp Cell Res 1:37–80
6. Fukuda T, Dong L (2003) Assembly of nanodevices with carbon nanotubes through nanorobotic manipulations. Proc IEEE 91:1803–1818
7. Kleindiek S. Nanorobots for material science, biology and micro mounting. Kleindiek Nanotechnik Technical Report. http://www.nanotechnik.com/mm3a.html
8. Saeidpourazar R, Jalili N (2008) Towards fused vision and force robust feedback control of nanorobotic-based manipulation and grasping. Mechatron Int J 18:566–577
9. Baumgarten PK (1971) Electrostatic spinning of acrylic microfibers. J Colloid Interface Sci 36:71
10. Laxminarayana K, Jalili N (2005) Functional nanotube-based textiles: pathway to next generation fabrics with enhanced sensing capabilities. Textil Res J 75(9):670–680
11. Hiremath S, Jalili N (2006) Optimal control of electrospinning for fabrication of nonwoven textile-based sensors and actuators. In: Proceedings of 3rd international conference of textile research, Cairo, Egypt, April 2006
12. Saeidpourazar R, Jalili N (2009) Towards microcantilever-based force sensing and manipulation: modeling, control development and implementation. Int J Robot Res 28(4):464–483
13. Bashash S, Saeidpourazar R, Jalili N (2010) Development of a high-speed laser-free atomic force microscopy. Rev Sci Instrum 81-023707:1–9
14. Abramovitch DY, Anderson AB, Pao LY, Schitter G (2007) A tutorial on the mechanics dynamics and control of atomic force microscopes. In: Proceedings of the 2007 American control conference, New York, 11–13 July

http://www.springer.com/978-1-4614-2118-4

Nanorobotics
Current Approaches and Techniques
Mavroidis, C.; Ferreira, A. (Eds.)
2013, XIV, 467 p., Hardcover
ISBN: 978-1-4614-2118-4